The Asn 38−Cys 84 H-Bond in Plastocyanin

Francesco Musiani,[†] Paolo Carloni,*[,‡] and Stefano Ciurli*[,†]

Department of Agro-Environmental Science and Technology, University of Bologna, Viale Giuseppe Fanin 40, I-40127 Bologna, Italy, and International School for Advanced Studies (SISSA/ISAS) and INFM DEMOCRITOS Simulation Center, Via Beirut 2-4, I-34014 Trieste, Italy

Received: December 12, 2003; In Final Form: February 13, 2004

There exists increasing evidence that second-shell ligands might affect the electronic structure of metalloproteins. We address this issue in the context of plastocyanins, where an H-bond between the copper-bound Cys Sγ and a vicinal Asn NH is always observed. By performing multiple sequence alignments, we show the full conservancy of this vicinal Asn residue. By performing density functional theory (DFT) calculations on model systems, we show that inclusion of the Asn backbone affects the spin density distribution around the copper center in fair agreement with experimental data. Our calculations provide further support to the proposal that fully conserved outer shell ligands should be taken into account for a proper description of metal active sites in proteins.

Introduction

Plastocyanins are small (∼10 KDa) soluble proteins involved in electron-transfer processes occurring during photosynthesis in green algae, higher plants, and cyanobacteria.[1−5] They belong to a large class of blue-copper proteins, containing Cu in the active site.[6−9] Several X-ray[10−21] and NMR[22−28] structures are available in either oxidized or reduced forms containing, respectively, Cu(II) or Cu(I). The Cu ion is found in a so-called type-I center,[29] where the metal ion is strongly bound to two histidines Nδ and a cysteine Sγ, in addition to a fourth, weakly bound, methionine Sδ to complete a distorted tetrahedral coordination environment (Figure 1).

The knowledge gained from structural data, combined with mutagenesis experiments,[30] spectroscopic techniques,[31,32,62] and quantum-chemical calculations,[33−36] have provided a deep understanding of the electronic structure of the Cu center in type-I copper proteins in the oxidized state. In particular, quantum-chemical methods have established that the HOMO involves a π* interaction between the Cys Sγ 3p and the Cu $3d_{x^2-y^2}$ orbitals.[32] These conclusions were drawn by including the metal center and its immediate coordination environment in the model. Interestingly, however, a recent paper on the oxidized form of the blue-copper azurin has provided further insights into the electronic properties. By including in the model residues (namely Met44, Asn47, Phe111, Ser113, Gly116, Trp118, Met120, and Lys122) other than those bound to the metal ion (namely Gly45, His46, Cys112, His117, and Met-(Gln)121), Jaszewski and Jezierska have shown that the character of the unpaired electron is highly delocalized over His46, Asn47, Cys112, Tyr113, and His117.[37] Very recent papers on a variety of metalloproteins other than Cu proteins have pointed out that, generally speaking, the outer shell may affect structural and electronic properties of the metal site.[38−40]

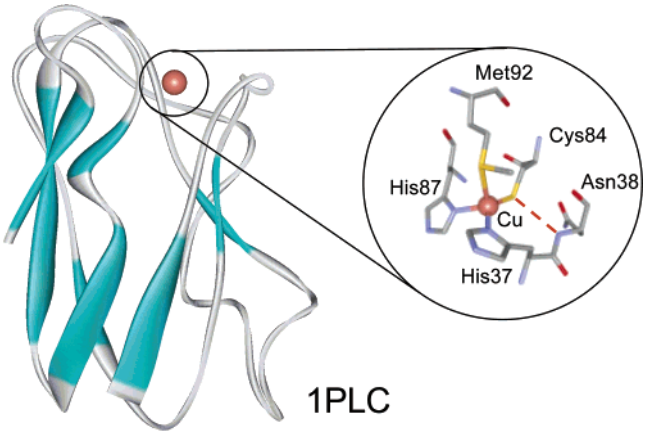

Figure 1. Structure of *Populus nigra* plastocyanin (PDB code 1PLC).[13] The β-strand characterizes the secondary structure (left panel). The copper site (right panel) shows the position of Asn38. The red dashed line indicates the presence of the H-bond between Cys84 Sγ and Asn38 NH. Atoms are colored according to the following scheme: copper, brown; carbon, gray; oxygen, red; nitrogen, blue; sulfur, yellow.

Here we focus on the role of the H-bond between the copper-bound Cys Sγ and a vicinal Asn NH, observed in all available plastocyanin structures (Table 1). The relevance of this structural feature has been pointed out by a variety of experiments on the Cu(II) protein, including paramagnetic ^{1}H NMR[27,41−43] and EPR[44] spectroscopies, as well as site-directed mutagenesis and visible spectroscopy.[30] These studies indicate a participation of this second-shell interaction in the electronic structure of the copper center.

We address the importance of this H-bond on the electronic structure of oxidized plastocyanins using a two-step approach. First, we perform a multiple sequence alignment of all plastocyanins so far sequenced and highlight the full conservancy of the vicinal Asn residue. Subsequently, we carry out an investigation of the role of the Asn NH−Cys Sγ H-bond by performing gradient-corrected DFT-B3LYP (density functional theory) calculations on model systems. In contrast to the previous calculations on a large model of azurin and including the second-shell ligands,[37] full geometry optimization is carried

* Corresponding authors. E-mail: carloni@sissa.it (P.C.); stefano.ciurli@unibo.it (S.C.). Phone: +39-040-378-7407 (P.C.); +39-051-209-6204 (S.C.). Fax: +39-040-378-7528 (P.C.); +39-051-209-6203 (S.C.).
[†] University of Bologna.
[‡] International School for Advanced Studies (SISSA/ISAS) and INFM DEMOCRITOS Simulation Center.

10.1021/jp037834z CCC: $27.50
Published on Web 05/05/2004

TABLE 1: Structural Parameters Related to the Asn N−Cys Sγ H-Bond in Plastocyanin Crystal Structures Available in the Protein Data Bank

PDB code	biological source	Cys no. consensus sequence	Asn no. consensus sequence	Asn N−Cys Sγ distance (Å)	Asn N−H−Cys Sγ angle (deg)[a]
1AG6	*S. oleracea* (ox)	38	84	3.45	163.3
1BAW	*P. laminosum* (ox)	40	89	3.74	163.7
1BXU	*Synechococcus* sp. (ox)	38	84	3.56	166.7
1BYO	*S. pratensis* (ox)	38	84	3.48	161.2
1IUZ	*U. petrusa* (ox)	38	84	3.62	163.3
1KDI	*D. crassirhizoma* (red)	38	87	3.48	171.1
1KDJ	*D. crassirhizoma* (ox)	38	87	3.41	171.9
1PCS	*Synechocystis* sp. (ox)	38	84	3.60	151.8
1PLC	*P. nigra* (ox)	38	84	3.50	157.5
1PNC	*P. nigra* (ox)	38	84	3.56	160.0
1PND	*P. nigra* (ox)	38	84	3.47	170.2
4PCY	*P. nigra* (red)	38	84	3.47	176.3
5PCY	*P. nigra* (red)	38	84	3.46	177.4
6PCY	*P. nigra* (red)	38	84	3.59	176.7
2PLT	*C. reinharditii* (ox)	38	84	3.56	165.5
7PCY	*E. prolifera* (red)	38	84	3.50	151.8

[a] When not present in the PDB file, the proton position was calculated assuming standard bond lengths and angles.

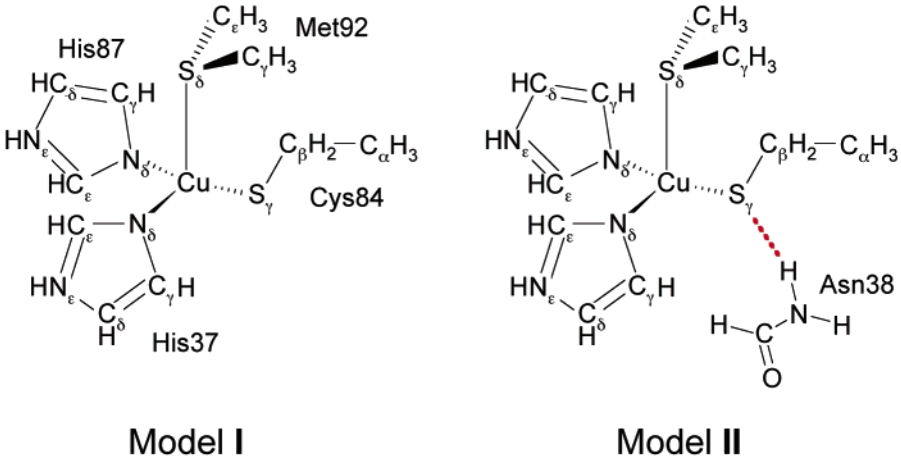

Figure 2. Schematic view of the models representing the plastocyanin copper site, as used in the calculations.

out using Gaussian (G) basis sets. Single-point calculations were then performed using both the Gaussian approach, as well as the BLYP level of theory using a plane wave (PW) basis set. The main outcome of our calculations is that the inclusion of the Asn backbone in the theoretical model affects the spin density distribution around the copper center, confirming, in general, the importance of the second-coordination shell for a full and more accurate description of the electronic properties of metal centers in metalloproteins.

Methods

Multiple Sequence Alignment. Sequences of plastocyanins were searched using sequence similarity criteria and the primary structure of *Populus nigra* (pople) plastocyanin as a template. The program FASTA3[45,46] available at the web address http://www.ebi.ac.uk/fasta[34] and the program BLAST (basic local alignment search tool)[47,48] available at http://www.ncbi.nlm.nih.gov/blast were utilized for the search. Plastocyanin sequences were retrieved from a nonredundant sum of different databases (SwissProt, TrEMBL, TrEMBLNew, GenBank CDS, PDB, PIR, PRF). Multiple sequence alignments were performed using the ClustalW program,[49] available at http://www.ebi.ac.uk/clustalw.

Quantum-Chemical Calculations. The metal center of plastocyanin was built using two different models (I and II in Figure 2). Model I represents the minimal copper coordination environment, whereas model II also includes the Asn NH−Cys Sγ hydrogen bond that is the object of this study. A molecule of formamide (FA) was used to model the protein backbone around the vicinal Asn residue. Models I and II were based on the crystal structure of oxidized *Populus nigra* plastocyanin (PDB entry 1PLC).[13] Histidines were modeled as imidazole rings, the cysteine anion as $CH_3CH_2S^-$, and methionine as $S(CH_3)_2$. Formamide was added in model II in the same position as the *Populus nigra* plastocyanin His37-Asn38 backbone fragment C(O)−N.

Geometry optimization of models I and II was carried out at the B3LYP[50,51] level of theory, using the quantum-chemical software Gaussian 98.[52] The following Gaussian (G) basis sets were used: (i) the Schäfer TZV basis set[53] for copper, (ii) the 6-311+G(d) basis set for the sulfur atoms, and (iii) the 6-31+G-(d) basis set for all other atoms. The local spin density (LSD) approximation was used. The nature of each critical point was characterized by computing the harmonic vibrational frequencies.

Calculations of the electronic structure were carried out using Gaussian 98 as well as CPMD 3.5.[54] In the latter case, the calculations were performed at the BLYP[51,63] level of theory on the B3LYP geometry-optimized structures for models I and II, using a basis set consisting of plane waves up to an energy cutoff of 80 Ry. Core/valence electron interactions were described using norm-conserving pseudopotentials of the Martin−Trouiller type.[55] A total of 2000 spline points were used for the description of the pseudopotentials. The models I and II were inserted in a cubic cell with edges of 15 and 17 Å,

Figure 3. ClustalW multiple sequence alignment of plastocyanin from (1) *Populus nigra*, (2) *Solano crispum*, (3) *Cucurbita pepo*, (4) *Solano tuberosum*, (5) *Copsella busra-pastoris*, (6) *Lycopersicon esculentum*, (7) *Nicotiana tabacum*, (8) *Mercurialis perennis*, (9) *Cucumis sativus*, (10) *Rumex obtusifolius*, (11) *Spinacea oleracea*, (12) *Lactuca sativa*, (13) *Phaseolus vulgaris*, (14) *Sambucus nigra*, (15) *Arabidopsis thaliana*, (16) *Vicia faba*, (17) *Pisum sativum*, (18) *Silene pratensis*, (19) *Fritillaria agrestis*, (20) *Oryza sativa*, (21) *Hordeum vulgare*, (22) *Petroselinum crispum*, (23) *Daucus carota*, (24) *Chlamydomonas reinhardtii*, (25) *Ulva petrusa*, (26) *Ulva arasakii*, (27) *Enteromorpha prolifera*, (28) *Scenedesmus obliquus*, (29) *Chlorella fusca*, (30) *Pediastrum boryanum*, (31) *Pyscommitrella patens*, (32) *Phormidium laminosum*, (33) *Synechocystis* sp. strain PCC6803, (34) *Anabena variabilis*, (35) *Anabena* sp. strain PCC7120, (36) *Anabena* sp. strain PCC7119, (37) *Prochlorothrix hollandia*, and (38) *Synechococcus* sp. strain PCC7942. The order in the alignment follows the ClustalW score. The conserved residues are highlighted with an asterisk (∗, 100% conservancy) or are reported in **bold** (100% conservancy, copper-binding residues) or *underlined italic* (the asparagine residue object of this study).

respectively, and they were treated as isolated systems following the procedure of Martyna and Tuckerman.[56]

Results and Discussion

Multiple Sequence Alignment. A protein sequence search was performed considering only native, nonredundant, sequences of plastocyanins, resulting in 38 hits. The sequences were aligned using ClustalW, and the results are reported in Figure 3. In this alignment the copper-binding residues, the vicinal Asn, and the other fully conserved residues are highlighted. The full conservation of the vicinal Asn, resulting from the multiple sequence alignment, is consistent with the large similarity of the structural parameters involving this H-bond of all available plastocyanin crystal structures (Table 1), underlining the key functional role for this residue, and suggesting similar structural features in all plastocyanins.

Quantum-Chemical Calculations. Models I and II were geometry-optimized at the B3LYP-G level of theory, and the electronic structure was investigated at both the B3LYP-G and BLYP-PW levels of theory. The geometry-optimized models are in good agreement with the experimental structures of oxidized plastocyanins (Table 2) and similar to that found by the B3LYP-G geometry optimization on the Cu coordination polyhedron.[35]

The main features of the electronic structure of model I, as obtained with both BLYP-PW and B3LYP-G calculations, reproduce previous results obtained by DFT calculations that used localized basis sets for the exchange correlation functionals.[32,35] In particular, the calculated HOMO involves a π^* orbital between Cu $3d_{x^2-y^2}$ and 3p of Cys84 Sγ (Figure 4A). The calculated unpaired spin density (SD) is localized essentially on the copper ion and the cysteine Sγ (Figure 4B and Table 3), consistent with sulfur K-edge[57] and copper L-edge[58] XAS spectroscopic studies.

In the G basis set calculation, the copper-bound Cys accounts for about 67% of the total SD, while the SD on the histidine residues is small for both residues (ca. 3%). The same is found in the PW calculation. These calculated values agree well with both ^{14}N ENDOR[59] and paramagnetic ^{1}H NMR data. As for the latter, the full assignment of the ^{1}H NMR spectra of oxidized plastocyanins from spinach[41] and *Synechocystis*[27] have allowed the determination of the corresponding Fermi contact shifts and

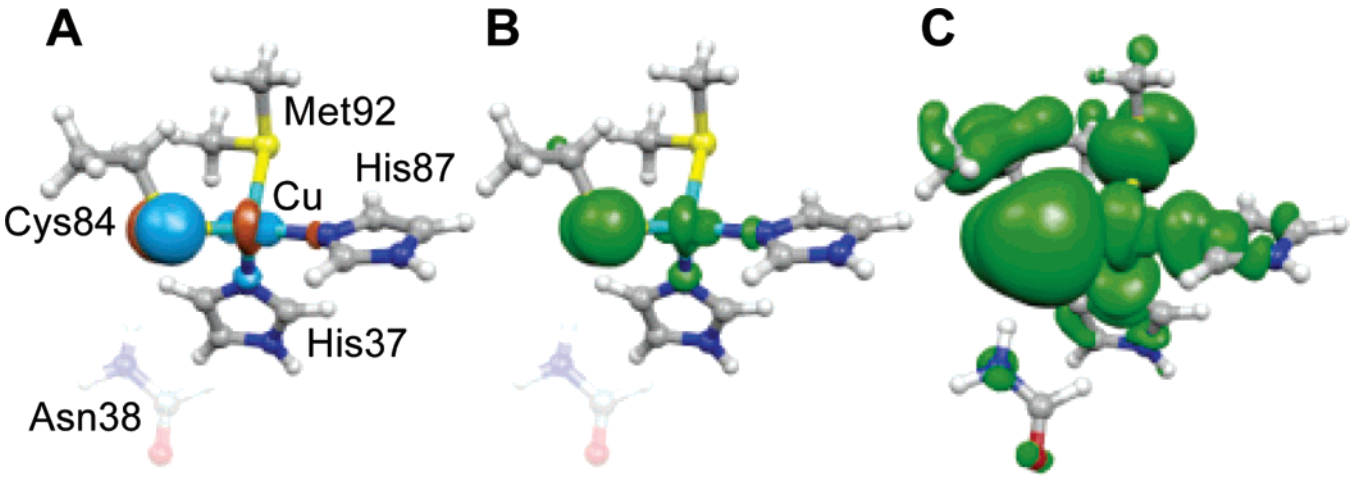

Figure 4. Depiction of the HOMO orbital of model I (panel A) and the corresponding spin density (panel B). The FA is showed dimmed. Panel C shows the spin density for model II, displayed in a lower threshold value in order to highlight the involvement of the vicinal peptide bond in the electronic structure. Atoms are colored according to the following scheme: copper, light blue; carbon, gray; oxygen, red; nitrogen, blue; sulfur, yellow.

TABLE 2: Selected Structural Parameters of Optimized Models and Crystal Structures of Oxidized Plastocyanin[a]

	plastocyanin oxidized	model I	model II
Cu−Nδ (His37)	1.89−2.22	2.02	2.08
Cu−Nδ (His87)	1.89−2.22	2.03	2.02
Cu−Sγ (Cys84)	2.07−2.21	2.19	2.21
Cu−Sδ (Met92)	2.78−2.91	2.90	2.80
Nδ (His37)−Cu−Nδ (His87)	96−104	104	103
Sγ (Cys84)−Cu−Sδ (Met92)	102−110	113	114
Nδ (His37)−Cu−Sγ (Cys84)	112−144	125	109
Nδ (His37)−Cu−Sδ (Met92)	85−108	98	98
Nδ (His87)−Cu−Sγ (Cyt84)	112−144	123	131
Nδ (His87)−Cu−Sδ (Met92)	85−108	93	97
Sγ (Cys84)−N (Asn38)	3.41−3.74		3.50
Cu−Sγ (Cys84)−N (Asn38)	108−114		104
Sγ (Cys84)−N (Asn38)−C (His37)	102−113		114
torsion Cu−Sγ (Cys84)−N (Asn38)−C (His37)	24−31		35

[a] Distances are in angstroms and angles are in degrees.

hyperfine coupling constants for the various nuclei around the oxidized Cu(II). These values are directly related to the delocalization of unpaired SD on the various nuclei,[60,61] and therefore can be compared to the values of SD calculated in the present theoretical study (see Table 3). In particular, the calculated SD on the Cys Hβ1 and Hβ2 protons corresponds very well to that estimated by ^{1}H NMR.[41]

The addition of the Asn NH−Cys Sγ H-bond (model II) affects to a small, albeit significant, extent the SD and the HOMO (Table 3). In particular, in both PW and G calculations, the SD and the HOMO character are increased on the copper ion and decreased on the Cys Sγ. In addition, the H-bond causes a small, yet significant, presence of spin density on the Cu-bound Met Sδ, consistent with the observed small ^{1}H NMR contact shifts for the Hγ protons of this residue in both spinach and cyanobacterial plastocyanin.[27,41] The most evident effect of the inclusion of the Asn backbone in the model is, however, the extension of the HOMO to include the pπ orbital of the peptide bond so that SD is present on both the N and O atoms of the Asn model. This result finally explains the observation of a sizable ^{1}H NMR negative hyperfine shift for the NH proton of the vicinal Asn involved in the H-bond with the Cu-bound Cys Sγ[27,41] as being due to a spin polarization mechanism by which the unpaired SD on the Asn N atom polarizes SD of opposite sign at the nucleus of the attached proton.[60,61] An improvement of the correspondence between the experimental

TABLE 3: Spin Density (Fraction of Electron) as Determined at the B3LYP-G Level

residue	atom	model I	model II	Δe	A_c[c]	A_c[d]
	Cu	0.266	0.294	0.028		
Cys84	Sγ	0.681	0.625	−0.056		
	Cβ	−0.040	−0.053	−0.013		
	Hβ1	0.016	0.020	0.004	23.2	21.9
	Hβ2	0.022	0.006	−0.016	17.4	18.4
	Cα	−0.005	0.020	0.025		
	Hα1	−0.001	0.001	0.002	−0.44	−0.4
	Hα2	0.000	0.000	0.000		
	Hα3	0.000	0.000	0.000		
His37	Nδ	0.028	0.030	0.002		
	Cγ	−0.001	−0.016	−0.015		
	Hγ	0.001	0.000	−0.001		
	Cδ	0.001	0.010	0.009		
	Hδ	0.000	0.000	0.000	1.45	1.6
	Nϵ	−0.001	−0.002	−0.001		
	NHϵ	0.001	0.000	−0.001	0.74	0.7
	Cϵ	−0.001	0.011	0.012		
	Hϵ	0.001	0.001	0.000	1.14	1.1
His87	Nδ	0.030	0.029	−0.001		
	Cγ	−0.018	−0.011	0.007		
	Hγ	0.000	0.000	0.000		
	Cδ	0.010	0.000	−0.010		
	Hδ	0.001	0.001	0.001	1.63	1.7
	Nϵ	−0.002	0.000	0.002		
	NHϵ	0.001	0.001	0.001		
	Cϵ	0.010	0.000	−0.010		
	Hϵ	0.001	0.001	0.000	1.01	1.1
Met92	Sδ	0.000	0.019	0.019		
	Cϵ	0.000	0.004	0.004		
	Hϵ1	0.000	0.001	0.001		
	Hϵ2	0.000	0.001	0.001		
	Hϵ3	0.000	0.000	0.000		
	Cγ	0.000	0.000	0.000		
	Hγ1	0.000	0.001	0.001	0.31	
	Hγ2	0.000	0.001	0.001	0.71	0.7
	Hγ3	0.000	0.000	0.000		
FA	N		0.001			
	NH [a]		0.000			
	NH [b]		0.000			
	C		0.000			
	O		0.001			
	H		0.000			

[a] FA hydrogen in the trans configuration with respect to the carbonylic oxygen. [b] FA hydrogen in the cis configuration. [c] Hyperfine coupling constant (MHz) calculated from the contact contribution to the hyperfine shift as determined by NMR in oxidized spinach plastocyanin.[41] [d] Hyperfine coupling constant (MHz) calculated from the contact contribution to the hyperfine shift as determined by NMR in oxidized *Synechocystis* sp. PCC6803 plastocyanin.[27]

and theoretical data might be attained by higher-level geometry optimizations and/or QM/MM methods on large models.

In conclusion, a fully conserved, second-shell ligand plays a role for the electronic properties of the metal center, confirming, in general, the importance of the second-coordination shell for a full and more accurate description of the electronic properties of the metal center in metalloproteins. This result is qualitatively observed using both the G or PW basis sets and is in general agreement with the results calculated for azurin,[37] obtained for a larger model than that used here but without carrying out full geometry optimization. These two studies suggest the general importance of the second-shell ligands in at least two type-I blue-copper proteins.

Acknowledgment. The authors thank Edgar Groenen for useful discussions and INFM for the computational resources. F.M. holds a jount MIUR-CIRMMP fellowship. The research was also supported by Grants from INTAS, INFM, and MIUR-PRIN 1999 and 2001 to S.C. and P.C.

References and Notes

(1) Redinbo, M. R.; Yeates, T. O.; Merchant, S. *J. Bioenerg. Biomembr.* **1994**, *26*, 49−66.
(2) Navarro, J. A.; Hervàs, M.; De la Rosa, M. A. *J. Biol. Inorg. Chem.* **1997**, *2*, 11−22.
(3) Sigfridsson, K. *Photosynth. Res.* **1998**, *57*, 1−28.
(4) Hope, A. B. *Biochim. Biophys. Acta* **2000**, *1456*, 5−26.
(5) Solomon, E. I.; Szilagyi, R. K.; DeBeer George, S.; Basumallick, L. *Chem. Rev.* **2004**, *104*, 419−458.
(6) Adman, E. T. *Adv. Protein Chem.* **1991**, *42*, 144−197.
(7) Sykes, A. G. *Struct. Bonding* **1991**, *75*, 175−224.
(8) Malmstrom, B. G. *Eur. J. Biochem.* **1994**, *223*, 711−718.
(9) Gray, H. B.; Malmstrom, B. G.; Williams, R. J. P. *J. Biol. Inorg. Chem.* **2000**, *5*, 551−559.
(10) Guss, J. M.; Freeman, H. C. *J. Mol. Biol.* **1983**, *169*, 521−563.
(11) Guss, J. M.; Harrowell, P. R.; Murata, M.; Norris, V. A.; Freeman, H. C. *J. Mol. Biol.* **1986**, *192*, 361−387.
(12) Collyer, C. A.; Guss, J. M.; Sugimura, Y.; Yoshizaki, F.; Freeman, H. C. *J. Mol. Biol.* **1990**, *211*, 617−632.
(13) Guss, J. M.; Bartunik, H. D.; Freeman, H. C. *Acta Crystallogr.* **1992**, *B48*, 790−811.
(14) Redinbo, M. R.; Cascio, D.; Choukair, M. K.; Rice, D.; Merchant, S.; Yeates, T. O. *Biochemistry* **1993**, *32*, 10560−10567.
(15) Xue, Y.; Okvist, M.; Hansson, O.; Young, S. *Protein Sci.* **1998**, *7*, 2099−2105.
(16) Shibata, N.; Inoue, T.; Nagano, C.; Nishio, N.; Kohzuma, T.; Onodera, K.; Yoshizaki, F.; Sugimura, Y.; Kai, Y. *J. Biol. Chem.* **1999**, *274*, 4225−4230.
(17) Romero, A.; De la Cerda, B.; Vareda, P. F.; Navarro, J. A.; Hervas, M.; De la Rosa, M. A. *J. Mol. Biol.* **1998**, *275*, 327−336.
(18) Kohzuma, T.; Inoue, T.; Yoshizaki, F.; Sasakawa, Y.; Onodera, K.; Nagatomo, S.; Kitagawa, T.; Uzawa, S.; Isobe, Y.; Sugimura, Y.; Gotowda, M.; Kai, Y. *J. Biol. Chem.* **1999**, *274*, 11817.
(19) Sugawara, H.; Inoue, T.; Li, C.; Gotowda, M.; Hibino, T.; Takabe, T.; Kai, Y. *J. Biochem. (Tokyo)* **1999**, *125*, 899−903.
(20) Inoue, T.; Sugawara, H.; Hamanaka, S.; Tsukui, H.; Suzuki, E.; Kohzuma, T.; Kai, Y. *Biochemistry* **1999**, *38*, 6063−6069.
(21) Bond, C. S.; Bendall, D. S.; Freeman, H. C.; Guss, J. M.; Howe, C. J.; Wagner, M. J.; Wilce, M. C. *Acta Crystallogr.* **1999**, *D55*, 414−421.
(22) Moore, J. M.; Lepre, C. A.; Gippert, J. P.; Chazin, W. J.; Case, D. A.; Wright, P. E. *J. Mol. Biol.* **1991**, *221*, 533−555.
(23) Bagby, S.; Driscoll, P. C.; Harvey, T. S.; Hill, H. A. O. *Biochemistry* **1994**, *33*, 6611−6622.
(24) Badsberg, U.; Jorgensen, A. M. M.; Gesmar, H.; Led, J. J.; Hammerstad, J. M.; Jespersen, L. L.; Ulstrup, J. *Biochemistry* **1996**, *35*, 7021−7031.
(25) Babu, C. R.; Volkman, B. F.; Bullerjahn, G. S. *Biochemistry* **1999**, *38*, 4988−4995.
(26) Ma, L.; Jorgensen, A.-M. M.; Sorensen, G. O.; Ulstrup, J.; Led, J. J. *J. Am. Chem. Soc.* **2000**, *122*, 9473−9485.
(27) Bertini, I.; Ciurli, S.; Dikiy, A.; Fernandez, C.; Luchinat, C.; Safarov, N.; Shumilin, S.; Vila, A. *J. Am. Chem. Soc.* **2001**, *123*, 2405−2413.
(28) Bertini, I.; Bryant, D. A.; Ciurli, S.; Dikiy, A.; Fernandez, C.; Luchinat, C.; Safarov, N.; Shumilin, S.; Vila, A. J.; Zhao, J. *J. Biol. Chem.* **2001**, *276*, 47217.
(29) Freeman, H. C.; Guss, J. M. In *Handbook of Metalloproteins*; Messerschmidt, A., Huber, R., Wieghardt, K., Poulos, T., Eds.; Wiley: New York, 2001.
(30) Dong, S.; Ybe, J. A.; Hecht, M. H.; Spiro, T. G. *Biochemistry* **1999**, *38*, 3379−3385.
(31) Holm, R. H.; Kennepohl, P.; Solomon, E. I. *Chem. Rev.* **1996**, *96*, 2239−2314.
(32) Randall, D. W.; Gamelin, D. R.; LaCroix, L. B.; Solomon, E. I. *J. Biol. Inorg. Chem.* **2000**, *5*, 16−29.
(33) Ryde, U.; Olsson, M. H.; Pierloot, K.; Roos, B. O. *J. Mol. Biol.* **1996**, *261*, 586−596.
(34) Olsson, M. H.; Ryde, U. *J. Biol. Inorg. Chem.* **1999**, *4*, 654−663.
(35) Ryde, U.; Olsson, M. H.; Roos, B. O.; De Kerpel, J. O.; Pierloot, K. *J. Biol. Inorg. Chem.* **2000**, *5*, 565−574.
(36) Szilagyi, R. K.; Solomon, E. I. *Curr. Opin. Chem. Biol.* **2002**, *6*, 250−258.
(37) Jaszewski, A. R.; Jezierska, J. *Chem. Phys. Lett.* **2001**, *343*, 571−580.
(38) Dudev, T.; Lin, Y.-I.; Dudev, M.; Lim, C. *J. Am. Chem. Soc.* **2003**, *125*, 3168−3180.
(39) Gervasio, F. L.; Schettino, V.; Mangani, S.; Krack, M.; Carloni, P.; Parrinello, M. *J. Phys. Chem B* **2003**, *107*, 6886−6892.
(40) Dal Peraro, M.; Vila, A. J.; Carloni, P. *J. Biol. Inorg. Chem.* **2002**, *7*, 704−712.
(41) Bertini, I.; Ciurli, S.; Dikiy, A.; Gasanov, R.; Luchinat, C.; Martini, G.; Safarov, N. *J. Am. Chem. Soc.* **1999**, *121*, 2037−2046.
(42) Bertini, I.; Fernandez, C. O.; Karlsson, B. G.; Leckner, J.; Luchinat, C.; Malmstrom, B. G.; Nersissian, A. M.; Pierattelli, R.; Shipp, E.; Valentine, J. S.; Vila, A. J. *J. Am. Chem. Soc.* **2000**, *122*, 3701−3707.
(43) Sato, K.; Kohzuma, T.; Dennison, C. *J. Am. Chem. Soc.* **2003**, *125*, 2101−2112.
(44) van Gastel, M.; Nagano, Y.; Zondervan, R.; Canters, G. W.; Jeuken, L. J. C.; Warmerdan, G. C. M.; de Waal, E. C.; Groenen, E. J. J. *J. Phys. Chem. B* **2002**, *106*, 4018−4021.
(45) Pearson, W. R.; Lipman, D. J. *Proc. Natl. Acad. Sci. U.S.A.* **1988**, *85*, 2444−2448.
(46) Pearson, W. R. *Methods Enzymol.* **1990**, *183*, 63−98.
(47) Altschul, S. F.; Gish, W.; Miller, W.; Myers, E. W.; Lipman, D. J. *J. Mol. Biol.* **1990**, *215*, 403−410.
(48) Altschul, S. F.; Madden, T. L.; Schaffer, A. A.; Zhang, J.; Zhang, Z.; Miller, W.; Lipman, D. J. *Nucleic Acids Res.* **1997**, *25*, 3389−3402.
(49) Thompson, J. D.; Higgins, D. G.; Gibson, T. J. *Nucleic Acids Res.* **1994**, *22*, 4673−4680.
(50) Lee, C.; Yang, W.; Parr, R. G. *Phys. Rev. B* **1988**, *37*, 785−789.
(51) Becke, A. D. *J. Chem. Phys.* **1993**, *98*, 5648−5652.
(52) Frisch, M. J.; Trucks, G. W.; Schlegel, H. B.; Scuseria, G. E.; Robb, M. A.; Cheeseman, J. R.; Zakrzewski, V. G.; Montgomery J. A., J.; Stratmann, R. E.; Burant, J. C.; Dapprich, S.; Millam, J. M.; Daniels, A. D.; Kudin, K. N.; Strain, M. C.; Farkas, O.; Tomasi, J.; Barone, V.; Cossi, M.; Cammi, R.; Mennucci, B.; Pomelli, C.; Adamo, C.; Clifford, S.; Ochterski, J.; Petersson, G. A.; Ayala, P. Y.; Cui, Q.; Morokuma, K.; Rega, N.; Salvador, P.; Dannenberg, J. J.; Malick, D. K.; Rabuck, A. D.; Raghavachari, K.; Foresman, J. B.; Cioslowski, J.; Ortiz, J. V.; Baboul, A. G.; Stefanov, B. B.; Liu, G.; Liashenko, A.; Piskorz, P.; Komaromi, I.; Gomperts, R.; Martin, R. L.; Fox, D. J.; Keith, T.; Al-Laham, M. A.; Peng, C. Y.; Nanayakkara, A.; Challacombe, M.; Gill, P. M. W.; Johnson, B.; Chen, W.; Wong, M. W.; Andres, J. L.; Gonzalez, C.; Head-Gordon, M.; Replogle, E. S.; Pople, J. A. *Gaussian 98*; Gaussian, Inc.: Pittsburgh, PA, 2002.
(53) Schaefer, A.; Horn, H.; Ahlrichs, R. *J. Chem. Phys.* **1992**, *97*, 2571−2577.
(54) Hutter, J.; Alavi, A.; Deutsch, T.; Silvestri, W.; Parrinello, M. *CPMD MPI fur Festkorperforschung*, version 3.5; IBM Research Laboratory: Stuttgard and Zurich, 2000.
(55) Troullier, N.; Martins, J. L. *Phys. Rev. B: Condens. Matter* **1991**, *43*, 1993−2006.
(56) Martyna, G. J.; Tuckerman, M. E. *J. Chem. Phys.* **1999**, *110*, 2810−2821.
(57) Shadle, S. E.; Penner-Hahn, J. E.; Schugar, H. J.; Hedman, B.; Hodgson, K. O.; Solomon, E. I. *J. Am. Chem. Soc.* **1993**, *115*, 767−776.
(58) George, S. J.; Lowery, M. D.; Solomon, E. I.; Cramer, S. P. *J. Am. Chem. Soc.* **1993**, *115*, 2968−2969.
(59) Werst, M. M.; Davoust, C. E.; Hoffman, B. M. *J. Am. Chem. Soc.* **1991**, *113*, 1533−1538.
(60) Bertini, I.; Luchinat, C. *NMR of Paramagnetic Molecules in Biological Systems*; Benjamin-Cummings: Menlo Park, CA, 1986.
(61) Bertini, I.; Luchinat, C. *NMR of Paramagnetic Substances*; Elsevier: Amsterdam, 1996; Vol. 150.
(62) Hansen, D. F.; Led, J. J. *J. Am. Chem. Soc.* **2004**, *126*, 1247−1252.
(63) Becke, A. D. *Phys. Rev. A* **1988**, *38*, 3098−3100.